All-pass-based design of nearly-linear phase IIR low-pass differentiators

Goran Stančić[a], Ivan Krstić[b] and Stevica Cvetković[a]

[a] University of Niš, Faculty of Electronic Engineering, Aleksandra Medvedeva 14, 18000 Niš, Serbia; [b] University of Priština, Faculty of Technical Sciences, Kneza Miloša 7, 38220 Kosovska Mitrovica, Serbia

ARTICLE HISTORY
Compiled November 14, 2019

ABSTRACT
A new approach to the design of the nearly-linear phase infinite impulse response low-pass differentiators using a parallel all-pass structure is discussed in this paper. The magnitude and phase responses of the proposed low-pass differentiators are first formulated as functions of the phase responses of the corresponding all-pass filters, and a set of equations is derived such that the magnitude response approximates the ideal one in the weighted Chebyshev sense both in the passband and the stopband. The maximum passband phase response linearity error is shown to be related to the maximum passband magnitude error and the value of an additional design parameter. Comparison with the existing nearly-linear phase infinite impulse response low-pass differentiators shows that the low-pass differentiators designed using the proposed method usually require less multiplications, which comes at the cost of a somewhat higher filter order and consequently higher group delay. However, as the reduced number of multiplications lead to lower power consumption if hardware implementation is considered, the proposed low-pass differentiators are an attractive alternative in applications where low group delay is not of crucial importance.

KEYWORDS
All-pass digital filter; parallel connection; weighted Chebyshev approximation; low-pass differentiators; nearly-linear phase response

1. Introduction

Low-pass differentiators, needed in various applications (Ferdi, 2010; Laguna, Thakor, Caminal & Jane, 1990; Luo, Bai, He & Ying, 2004; Platas-Garza, Platas-Garza & de la O Serna, 2009; Skolnik, 1980; Väliviita & Ovaska, 1998; Wulf, Staude, Knopp & Felderhoff, 2016) where the time derivative of the input signal at low frequencies is of interest, while high frequency noise needs to be suppressed, can be designed either as a finite impulse response (Ferdi, 2010; Khan, Okuda & Ohba, 2005; Kumar & Roy, 1988; de la O Serna & Platas-Garza, 2011; Selesnick, 2002; Wang, 2013; Wulf et al., 2016) or an infinite impulse response (IIR) filters (Al-Alaoui, 1995, 2007; Le Bihan, 1993; Nakamoto & Ohno, 2014; Nongpiur, Shpak & Antoniou, 2014; Skogstad, Holm & Høvin, 2012; Stančić, Krstić & Živković, 2019; Yoshida, Nakamoto & Aikawa, 2018). While a perfectly linear passband phase response of an IIR low-pass differentiator

CONTACT Ivan Krstić. Email: ivan.krstic@pr.ac.rs

cannot be achieved, the order of a IIR low-pass differentiator is significantly lower compared to its finite impulse response counterpart. Furthermore, in most applications the fact that the passband phase response is not perfectly linear is not an issue if it is a nearly-linear function of frequency.

There are several approaches to IIR low-pass differentiators design. The conventional approach is based on the cascade connection of the fullband differentiator and the appropriate low-pass filter (Skogstad et al., 2012; Stančić et al., 2019). On the other hand, IIR low-pass differentiators in (Al-Alaoui, 1995; Le Bihan, 1993) are designed by inverting the transfer function of the IIR low-pass integrators, followed by reflection of the unstable poles inside the unit circle. The methods of the third approach (Al-Alaoui, 2007; Nakamoto & Ohno, 2014; Nongpiur et al., 2014; Skogstad et al., 2012; Yoshida et al., 2018) formulate the IIR low-pass differentiator design problem as a constrained optimization problem. In (Al-Alaoui, 2007; Skogstad et al., 2012), the numerator of the IIR low-pass differentiator is assumed to be the linear-phase filter while the denominator coefficients are obtained using the classical (Al-Alaoui, 2007) and metaheuristic (Skogstad et al., 2012) constrained optimization methods. Another constrained optimization IIR low-pass differentiator design method that minimises the group-delay deviation of the IIR low-pass differentiator with respect to the average group delay under the constraints that the maximum relative passband magnitude response error and maximum average squared stopband magnitude response are below the prescribed values is proposed in (Nongpiur et al., 2014), while the design method presented in (Nakamoto & Ohno, 2014; Yoshida et al., 2018) formulates the IIR low-pass differentiator design problem in quadratic form without frequency sampling, such that magnitude and phase response specifications are simultaneously approximated.

In a recently published paper (Stančić et al., 2019), the authors reported an all-pass-based design of IIR fullband differentiators. In the paper, this concept is extended towards the design of nearly-linear phase IIR low-pass differentiators whose magnitude response approximates the ideal one in the weighted Chebyshev sense. The novelty of the paper is the introduction of a new structure for the IIR low-pass differentiators design composed of two parallel all-pass filters of the same orders, where one of the all-pass branches is a pure delay. Furthermore, the maximum passband phase response linearity error of the proposed low-pass differentiators is shown to be related to the maximum passband magnitude error and the value of an additional design parameter; therefore it can be effectively controlled. To the best of our knowledge, the design of IIR low-pass differentiators using a parallel all-pass structure has not been considered in the existing literature.

The rest of the paper is structured as follows. The problem formulation of the all-pass-based nearly-linear phase IIR low-pass differentiator with magnitude response approximating the ideal one in the weighted Chebyshev sense is given in Sec. 2. The proposed IIR low-pass differentiator design method is presented in Sec. 3, while considerations regarding the relative passband magnitude error minimization are given in Sec. 4. Design examples along with a comparison with the existing nearly-linear phase IIR low-pass differentiators are discussed in Sec. 5, while concluding remarks are drawn in Sec. 6.

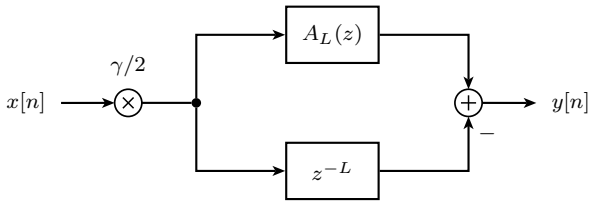

Figure 1. Low-pass differentiator realised using parallel all-pass structure.

2. Problem formulation

The transfer function of IIR low-pass differentiators, whose design is considered in this paper, is assumed to take the following form

$$H(z) = \frac{\gamma}{2}\left[A_L(z) - z^{-L}\right], \tag{1}$$

as shown in Figure 1, where $A_L(z)$ is the transfer function of the Lth order stable all-pass transfer function with single poles

$$A_L(z) = z^{-L}\frac{1 + \sum_{i=1}^{L} a_i z^i}{1 + \sum_{i=1}^{L} a_i z^{-i}}. \tag{2}$$

The magnitude and phase responses of the proposed low-pass differentiator can easily be formulated as functions of the phase response of the all-pass filter $A_L(z)$, denoted by $\phi(\omega)$, by substituting $z = e^{j\omega}$ in (1), followed by some mathematical manipulations

$$\left|H\left(e^{j\omega}\right)\right| = \gamma\left|\sin\frac{\phi(\omega) + L\omega}{2}\right|, \tag{3a}$$

$$\varphi(\omega) = \arg\left\{H\left(e^{j\omega}\right)\right\} = \frac{\phi(\omega) - L\omega + \pi}{2}, \tag{3b}$$

while $\phi(\omega)$ can be determined from (2) as

$$\phi(\omega) = -L\omega + 2\arctan\frac{\sum_{i=1}^{L} a_i \sin(i\omega)}{1 + \sum_{i=1}^{L} a_i \cos(i\omega)}. \tag{4}$$

As the phase response $\phi(\omega)$ of the stable real Lth order all-pass filter transfer function, $A_L(z)$, satisfies $\phi(0) = 0$ and $\phi(\pi) = -L\pi$, from (3a) it follows that $\left|H\left(e^{j0}\right)\right| = 0$ and $\left|H\left(e^{j\pi}\right)\right| = 0$.

The frequency response of an ideal low-pass differentiator having a nonzero transition region width takes the following form

$$H_{\mathrm{id}}\left(e^{j\omega}\right) = \begin{cases} j\omega e^{-j\omega\tau}, & \omega \le \omega_p \\ 0, & \omega \ge \omega_s \end{cases}, \tag{5}$$

where ω_p and $\omega_s > \omega_p$ are passband and stopband edge frequencies, respectively, while τ is the passband group delay. The magnitude response of the proposed IIR low-pass differentiators, (3a), approximates the ideal one which from (5) can be derived as

$$\left|H_{\mathrm{id}}\left(e^{j\omega}\right)\right| = \begin{cases} \omega, & \omega \le \omega_p \\ 0, & \omega \ge \omega_s \end{cases}, \tag{6}$$

if $\phi(\omega)$ approximates either

$$\phi'(\omega) = \begin{cases} -L\omega + 2\arcsin\frac{\omega}{\gamma}, & \omega \le \omega_p \\ -L\omega, & \omega \ge \omega_s \end{cases}, \tag{7}$$

or

$$\phi''(\omega) = \begin{cases} -L\omega - 2\arcsin\frac{\omega}{\gamma}, & \omega \le \omega_p \\ -L\omega, & \omega \ge \omega_s \end{cases}. \tag{8}$$

However, for a narrow transition region, $\phi''(\omega_p)$ is less than $\phi''(\omega_s)$, which cannot be achieved by the stable all-pass filter $A_L(z)$, since its phase response is a monotonically decreasing function of frequency. To circumvent this situation, it will be assumed that the all-pass filter phase response $\phi(\omega)$ approximates $\phi'(\omega)$. To ensure the monotonically decreasing behavior of $\phi'(\omega)$, the following should be satisfied

$$\frac{\mathrm{d}\phi'(\omega)}{\mathrm{d}\omega} < 0, \tag{9}$$

which is equivalent to

$$\gamma > \omega_p\sqrt{1 + \left(\frac{2}{L\omega_p}\right)^2}. \tag{10}$$

Since the phase response approximation error function of the all-pass filter $A_L(z)$ equals

$$\zeta_\phi(\omega) = \phi(\omega) - \phi'(\omega) = \begin{cases} \phi(\omega) + L\omega - 2\arcsin\frac{\omega}{\gamma}, & \omega \le \omega_p \\ \phi(\omega) + L\omega, & \omega \ge \omega_s \end{cases}, \tag{11}$$

the magnitude response of the proposed IIR low-pass differentiator, given by (3a), in the passband and the stopband can be formulated as

$$\left|H\left(e^{j\omega}\right)\right| = \begin{cases} \gamma\left|\sin\left(\arcsin\frac{\omega}{\gamma} + \frac{\zeta_\phi(\omega)}{2}\right)\right|, & \omega \le \omega_p \\ \gamma\left|\frac{\sin\zeta_\phi(\omega)}{2}\right|, & \omega \ge \omega_s \end{cases}. \tag{12}$$

Adopting the assumption that the phase response approximation error of the all-pass filter $A_L(z)$ satisfies the inequality

$$\zeta_\phi(\omega) > -2\arcsin\frac{\omega}{\gamma}, \quad 0 < \omega \le \omega_p, \tag{13}$$

(12), and consequently (3a) can be rewritten as

$$\left|H\left(e^{j\omega}\right)\right| = \begin{cases} \gamma \sin \frac{\phi(\omega)+L\omega}{2}, & \omega \leq \omega_p \\ \gamma \left|\sin \frac{\phi(\omega)+L\omega}{2}\right|, & \omega \geq \omega_s \end{cases} . \tag{14}$$

Based on the previous discussion it can be concluded that the proposed IIR low-pass differentiator exhibits a magnitude response approximating the ideal one in the weighted Chebyshev sense both in the passband and the stopband if the magnitude response error function

$$\xi(\omega) = W(\omega)\left(\left|H\left(e^{j\omega}\right)\right| - \left|H_{\mathrm{id}}\left(e^{j\omega}\right)\right|\right), \tag{15}$$

satisfies

$$\xi(\widetilde{\omega}_k) = W(\widetilde{\omega}_k)\left[\gamma \sin \frac{\phi(\widetilde{\omega}_k) + L\widetilde{\omega}_k}{2} - \widetilde{\omega}_k\right] = (-1)^{k+m}\delta_p, \tag{16}$$

for $k = 1, 2, \ldots, m$, and

$$(-1)^k \xi(\widehat{\omega}_k) = \gamma W(\widehat{\omega}_k) \sin \frac{\phi(\widehat{\omega}_k) + L\widehat{\omega}_k}{2} = (-1)^k \delta_s, \tag{17}$$

for $k = 1, 2, \ldots, L - m$, while at the passband and the stopband edge frequencies

$$\xi(\omega_p) = W(\omega_p)\left[\gamma \sin \frac{\phi(\omega_p) + L\omega_p}{2} - \omega_p\right] = -\delta_p, \tag{18a}$$

$$\xi(\omega_s) = \gamma W(\omega_s) \sin \frac{\phi(\omega_s) + L\omega_s}{2} = \delta_s, \tag{18b}$$

where δ_p and δ_s are passband and stopband weighted Chebyshev norms, respectively,

$$\delta_p = \max_{\omega \leq \omega_p} \left|\xi(\omega)\right|, \tag{19a}$$

$$\delta_s = \max_{\omega \geq \omega_s} \xi(\omega), \tag{19b}$$

$W(\omega)$ is the positive weighting function, m is the number of sign-alternating extremal values in the passband, while the frequencies where extremal values occur are $0 \leq \widetilde{\omega}_1 < \widetilde{\omega}_2 < \cdots < \widetilde{\omega}_m < \omega_p$ and $\omega_s < \widehat{\omega}_1 < \widehat{\omega}_2 < \cdots < \widehat{\omega}_{L-m} < \pi$. The graphical interpretation of the IIR low-pass differentiator's magnitude response approximating the ideal one in the weighted Chebyshev sense is shown in Figure 2.

Regarding the passband phase response of the proposed low-pass differentiators, substitution of (11) in (3b) yields

$$\varphi(\omega) = \frac{\pi}{2} - L\omega + \arcsin\frac{\omega}{\gamma} + \frac{\zeta_\phi(\omega)}{2}, \quad \omega \leq \omega_p, \tag{20}$$

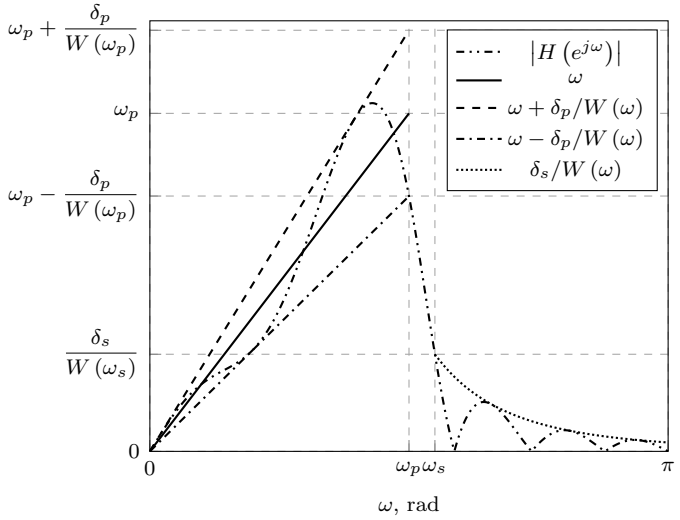

Figure 2. Graphical interpretation of the IIR low-pass differentiator's magnitude response approximating the ideal one in the weighted Chebyshev sense both in the passband and the stopband, for $L = 6$, $m = 3$.

which for $\gamma \gg \omega_p$ reduces to

$$\varphi(\omega) \approx \frac{\pi}{2} - \omega\left(L - \gamma^{-1}\right) + \frac{\zeta_\phi(\omega)}{2}, \quad \omega \leq \omega_p. \tag{21}$$

Obviously, the passband phase response of the proposed IIR low-pass differentiators is a nearly-linear function of frequency for a small all-pass filter's $A_L(z)$ passband phase response approximation error and γ sufficiently greater than the passband edge frequency ω_p.

2.1. Passband phase response linearity error of the proposed low-pass differentiators

Denoting the average passband group delay of the low-pass differentiator by

$$\overline{\tau} = \frac{1}{\omega_p}\int_0^{\omega_p} \tau(\omega)\,\mathrm{d}\omega = \frac{\varphi(0) - \varphi(\omega_p)}{\omega_p}, \tag{22}$$

the passband phase response linearity error defined as (Nongpiur et al., 2014):

$$\zeta_\varphi(\omega) = \varphi(\omega) - \left(\frac{\pi}{2} - \omega\overline{\tau}\right), \tag{23}$$

in case of the proposed low-pass differentiators, that is, by employing (3b) and (18a), can be formulated in terms of the phase response $\phi(\omega)$ of the corresponding all-pass filter $A_L(z)$, the passband weighted Chebyshev norm δ_p and the value of the parameter γ as

$$\zeta_\varphi(\omega) = \frac{\phi(\omega) + L\omega}{2} - \frac{\omega}{\omega_p}\arcsin\left[\gamma^{-1}\left(\omega_p - \frac{\delta_p}{W(\omega_p)}\right)\right]. \tag{24}$$

Since from (19a) it follows that

$$\arcsin\left[\gamma^{-1}\left(\omega-\frac{\delta_p}{W(\omega)}\right)\right]\leq\frac{\phi(\omega)+L\omega}{2}\leq\arcsin\left[\gamma^{-1}\left(\omega+\frac{\delta_p}{W(\omega)}\right)\right],\qquad(25)$$

for $\omega\leq\omega_p$, it can be concluded that the passband phase response linearity error of the proposed low-pass differentiators satisfies

$$\mathcal{L}(\omega)\leq\zeta_\varphi(\omega)\leq\mathcal{U}(\omega),\qquad(26)$$

where the lower and upper margin functions of the passband phase response linearity error are equal to

$$\mathcal{L}(\omega)=\arcsin\left[\gamma^{-1}\left(\omega-\frac{\delta_p}{W(\omega)}\right)\right]-\frac{\omega}{\omega_p}\arcsin\left[\gamma^{-1}\left(\omega_p-\frac{\delta_p}{W(\omega_p)}\right)\right],\qquad(27a)$$

$$\mathcal{U}(\omega)=\arcsin\left[\gamma^{-1}\left(\omega+\frac{\delta_p}{W(\omega)}\right)\right]-\frac{\omega}{\omega_p}\arcsin\left[\gamma^{-1}\left(\omega_p-\frac{\delta_p}{W(\omega_p)}\right)\right].\qquad(27b)$$

3. Design method

In this section, an iterative procedure for determination of the unknown all-pass filter coefficient vector

$$\boldsymbol{a}=[a_1,\,a_2,\,\ldots,\,a_L]^T,\qquad(28)$$

such that the obtained magnitude response of the IIR low-pass differentiator approximates the ideal one in the weighted Chebyshev sense both in the passband and the stopband is discussed. Determination of the initial solution for the coefficient vector $\boldsymbol{a}^{(0)}$, such that $\xi\left(\omega,\,\boldsymbol{a}^{(0)}\right)$ exhibits L extremal values, is discussed first.

3.1. Determination of the initial solution for the coefficient vector

Since the initial solution for the all-pass filter $A_L(z)$ coefficient vector $\boldsymbol{a}^{(0)}$ should be determined such that the magnitude response error function $\xi\left(\omega,\,\boldsymbol{a}^{(0)}\right)$ exhibit m and $L-m$ extremal values in the passband and the stopband, respectively, it is determined by setting the all-pass filter's $A_L(z)$ phase response approximation error function $\zeta_\phi\left(\omega,\,\boldsymbol{a}^{(0)}\right)$ to zero value at L distinct frequency points:

$$\omega'_k=k\frac{\omega_p}{m+1},\quad k=1,\,2,\,\ldots,\,m,\qquad(29a)$$

$$\omega''_k=\omega_s+k\frac{\pi-\omega_s}{L-m+1},\quad k=1,\,2,\,\ldots,\,L-m,\qquad(29b)$$

which is equivalent to

$$\phi\left(\omega'_k,\, \boldsymbol{a}^{(0)}\right) = \phi'\left(\omega'_k\right) = -L\omega'_k + 2\arcsin\frac{\omega'_k}{\gamma}, \quad k = 1,\, 2,\, \ldots,\, m, \tag{30a}$$

$$\phi\left(\omega''_k,\, \boldsymbol{a}^{(0)}\right) = \phi'\left(\omega''_k\right) = -L\omega''_k, \quad k = 1,\, 2,\, \ldots,\, L-m. \tag{30b}$$

Since phase response $\phi(\omega)$ of the all-pass filter $A_L(z)$ is related to its coefficients as

$$\sum_{i=1}^{L} a_i \sin\frac{\phi(\omega) + (L-2i)\,\omega}{2} = -\sin\frac{\phi(\omega) + L\omega}{2}, \tag{31}$$

note (4), (30) can be rewritten in matrix notation as

$$\boldsymbol{\Upsilon}\boldsymbol{a}^{(0)} = \boldsymbol{\eta}, \tag{32}$$

where $\boldsymbol{\Upsilon} = [\upsilon_{ki}]$ is the $L \times L$ square matrix, while $\boldsymbol{\eta} = [\eta_k]$ is the $L \times 1$ column vector such that

$$\upsilon_{ki} = \begin{cases} \sin\left(i\omega'_k - \arcsin\frac{\omega'_k}{\gamma}\right), & 1 \le k \le m \\ \sin\left(i\omega''_{k-m}\right), & m+1 \le k \le L \end{cases}, \tag{33a}$$

$$\eta_k = \begin{cases} \gamma^{-1}\omega'_k, & 1 \le k \le m \\ 0, & m+1 \le k \le L \end{cases}. \tag{33b}$$

Therefore, the solution for $\boldsymbol{a}^{(0)}$ can be determined as

$$\boldsymbol{a}^{(0)} = \boldsymbol{\Upsilon}^{-1}\boldsymbol{\eta}. \tag{34}$$

All-pass filter phase response error functions $\zeta_\phi\left(\omega,\, \boldsymbol{a}^{(0)}\right)$ and the corresponding magnitude response error functions $\xi\left(\omega,\, \boldsymbol{a}^{(0)}\right)$ for $L = 4,\, 6$, $W(\omega) = 1$, $\gamma = 4$, $m = \lfloor (L+1)/2 \rfloor$, $\omega_p = 0.4\pi$ and $\omega_s = 0.6\pi$ are shown in Figure 3.

3.2. Proposed algorithm

In every iteration $t \ge 1$ of the algorithm, the coefficient vector $\boldsymbol{a}^{(t)}$ and the values of the parameters $\delta_p^{(t)}$ and $\delta_s^{(t)}$ are obtained by means of the previously determined vector $\boldsymbol{a}^{(t-1)}$. The aforementioned is performed by solving approximately the following system of $L+2$ equations in $L+2$ unknowns (note (16), (17) and (18)):

$$\sin\frac{\phi\left(\widetilde{\omega}_k^{(t-1)},\, \boldsymbol{a}^{(t)}\right) + L\widetilde{\omega}_k^{(t-1)}}{2} = \frac{\widetilde{\omega}_k^{(t-1)}}{\gamma} + \frac{(-1)^{k+m}\,\delta_p^{(t)}}{\gamma W\left(\widetilde{\omega}_k^{(t-1)}\right)}, \quad k = 1,\, 2,\, \ldots,\, m, \tag{35a}$$

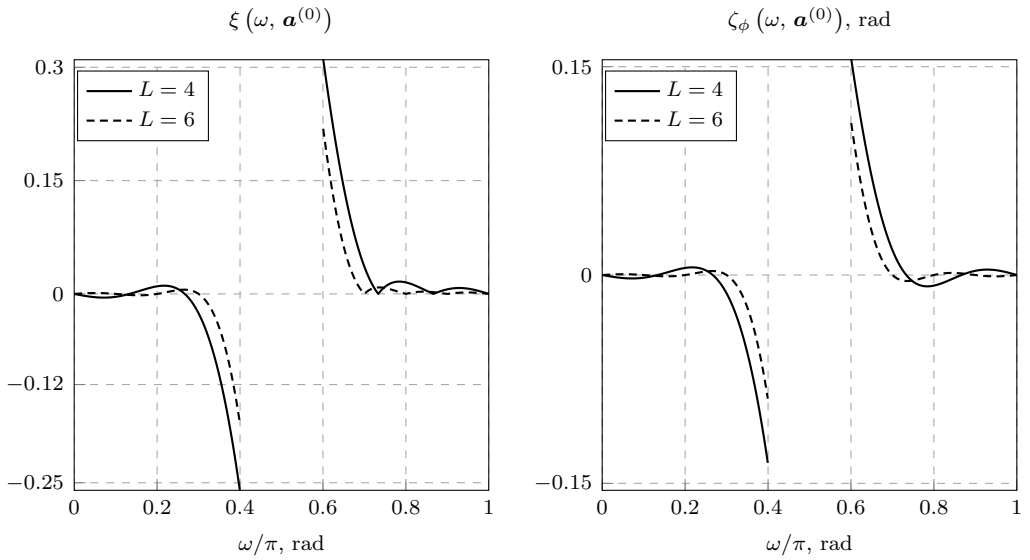

Figure 3. The magnitude response error function $\xi\left(\omega,\, \boldsymbol{a}^{(0)}\right)$ of the low-pass differentiator $H\left(z\right)$, and the corresponding phase response error function $\zeta_\phi\left(\omega,\, \boldsymbol{a}^{(0)}\right)$ of the all-pass filter $A_L\left(z\right)$, for $L = 4,\, 6$, $W\left(\omega\right) = 1$, $\gamma = 4$, $m = \lfloor\left(L+1\right)/2\rfloor$, $\omega_p = 0.4\pi$, $\omega_s = 0.6\pi$.

$$\sin\frac{\phi\left(\widehat{\omega}_k^{(t-1)},\, \boldsymbol{a}^{(t)}\right) + L\widehat{\omega}_k^{(t-1)}}{2} = \frac{\left(-1\right)^k \delta_s^{(t)}}{\gamma W\left(\widehat{\omega}_k^{(t-1)}\right)}, \quad k = 1,\, 2,\, \ldots,\, L-m, \tag{35b}$$

$$\sin\frac{\phi\left(\omega_p,\, \boldsymbol{a}^{(t)}\right) + L\omega_p}{2} = \frac{\omega_p}{\gamma} - \frac{\delta_p^{(t)}}{\gamma W\left(\omega_p\right)}, \tag{35c}$$

$$\sin\frac{\phi\left(\omega_s,\, \boldsymbol{a}^{(t)}\right) + L\omega_s}{2} = \frac{\delta_s^{(t)}}{\gamma W\left(\omega_s\right)}, \tag{35d}$$

where $\widetilde{\omega}_k^{(t-1)}$ and $\widehat{\omega}_k^{(t-1)}$ are frequency positions of the kth extremal point of the magnitude error function $\xi\left(\omega,\, \boldsymbol{a}^{(t-1)}\right)$ in the passband and the stopband, respectively. Namely, since the left-hand sides of the previous equations are nonlinear in the unknown coefficient vector $\boldsymbol{a}^{(t)} = \boldsymbol{a}^{(t-1)} + \Delta\boldsymbol{a}^{(t)}$, they are replaced by their first order Taylor expansions which take the following form

$$\sin\frac{\phi\left(\omega,\, \boldsymbol{a}^{(t)}\right) + L\omega}{2} = \sin\frac{\phi\left(\omega,\, \boldsymbol{a}^{(t-1)}\right) + L\omega}{2} + \sum_{i=1}^{L} \Delta a_i^{(t)} \cdot \frac{\partial}{\partial a_i} \sin\frac{\phi\left(\omega,\, \boldsymbol{a}^{(t-1)}\right) + L\omega}{2}, \tag{36}$$

where partial derivatives can be determined using (4) as

$$\frac{\partial}{\partial a_i}\sin\frac{\phi\left(\omega,\,\boldsymbol{a}^{(t-1)}\right)+L\omega}{2}=\cos\frac{\phi\left(\omega,\,\boldsymbol{a}^{(t-1)}\right)+L\omega}{2}\cdot\frac{\sin\left(i\omega\right)+\sum_{n=1}^{L}a_n^{(t-1)}\sin\left(\omega\left(i-n\right)\right)}{\left(1+\sum_{n=1}^{L}a_n^{(t-1)}\cos\left(n\omega\right)\right)^2+\left(\sum_{n=1}^{L}a_n^{(t-1)}\sin\left(n\omega\right)\right)^2}.\tag{37}$$

In this way, linearised forms of (35) can be rewritten in matrix notation as

$$\boldsymbol{\Psi}^{(t-1)}\cdot\begin{bmatrix}\Delta\boldsymbol{a}^{(t)}\\ \delta_p^{(t)}\\ \delta_s^{(t)}\end{bmatrix}=\boldsymbol{\lambda}^{(t-1)},\tag{38}$$

where $\boldsymbol{\Psi}^{(t-1)}=\left[\psi_{ki}^{(t-1)}\right]$ and $\boldsymbol{\lambda}^{(t-1)}=\left[\lambda_k^{(t-1)}\right]$ are the $(L+2)\times(L+2)$ square matrix and $(L+2)\times 1$ column vector, respectively, with elements

$$\psi_{ki}^{(t-1)}=\begin{cases}\gamma\frac{\partial}{\partial a_i}\sin\frac{\phi\left(\widetilde{\omega}_k^{(t-1)},\boldsymbol{a}^{(t-1)}\right)+L\widetilde{\omega}_k^{(t-1)}}{2}, & 1\le i\le L, \quad 1\le k\le m\\ \gamma\frac{\partial}{\partial a_i}\sin\frac{\phi\left(\widehat{\omega}_{k-m}^{(t-1)},\boldsymbol{a}^{(t-1)}\right)+L\widehat{\omega}_{k-m}^{(t-1)}}{2}, & 1\le i\le L, \quad m+1\le k\le L\\ \gamma\frac{\partial}{\partial a_i}\sin\frac{\phi\left(\omega_p,\boldsymbol{a}^{(t-1)}\right)+L\omega_p}{2}, & 1\le i\le L, \quad k=L+1\\ \gamma\frac{\partial}{\partial a_i}\sin\frac{\phi\left(\omega_s,\boldsymbol{a}^{(t-1)}\right)+L\omega_s}{2}, & 1\le i\le L, \quad k=L+2\\ (-1)^{k+m+1}W^{-1}\left(\widetilde{\omega}_k^{(t-1)}\right), & i=L+1, \quad 1\le k\le m\\ (-1)^{k-m+1}W^{-1}\left(\widehat{\omega}_{k-m}^{(t-1)}\right), & i=L+2, \quad m+1\le k\le L\\ W^{-1}\left(\omega_p\right), & i=L+1, \quad k=L+1\\ -W^{-1}\left(\omega_s\right), & i=L+2, \quad k=L+2\\ 0, & i=L+1, \quad m+1\le k\le L\\ 0, & i=L+2, \quad 1\le k\le m\\ 0, & i=L+1, \quad k=L+2\\ 0, & i=L+2, \quad k=L+1\end{cases},\tag{39a}$$

$$\lambda_k^{(t-1)}=\begin{cases}\widetilde{\omega}_k^{(t-1)}-\gamma\sin\frac{\phi\left(\widetilde{\omega}_k^{(t-1)},\boldsymbol{a}^{(t-1)}\right)+L\widetilde{\omega}_k^{(t-1)}}{2}, & 1\le k\le m\\ -\gamma\sin\frac{\phi\left(\widehat{\omega}_{k-m}^{(t-1)},\boldsymbol{a}^{(t-1)}\right)+L\widehat{\omega}_{k-m}^{(t-1)}}{2}, & m+1\le k\le L\\ \omega_p-\gamma\sin\frac{\phi\left(\omega_p,\boldsymbol{a}^{(t-1)}\right)+L\omega_p}{2}, & k=L+1\\ -\gamma\sin\frac{\phi\left(\omega_s,\boldsymbol{a}^{(t-1)}\right)+L\omega_s}{2}, & k=L+2\end{cases}.\tag{39b}$$

Based on the above discussion, an approximate solution for $\boldsymbol{a}^{(t)}$ can be obtained by solving the system of linear equations given by (38). On the other hand, the obtained solution does not guarantee that extremal values of the proposed recursive low-pass differentiator's magnitude response error function occur at frequencies $\widetilde{\omega}_k^{(t-1)}$, for $1\le k\le m$, and $\widehat{\omega}_k^{(t-1)}$, for $1\le k\le L-m$. Hence, an exchange algorithm for the IIR low-pass differentiator design is proposed:

(1) Set $t = 0$, $\delta_p^{(0)} = 0$, $\delta_s^{(0)} = 0$. Determine $\boldsymbol{a}^{(0)}$ using (34).
(2) Update current iteration, i.e. $t = t + 1$.
(3) Based on the known coefficient vector $\boldsymbol{a}^{(t-1)}$ determine the set of frequencies $\widetilde{\omega}_k^{(t-1)}$, $1 \leq k \leq m$, and $\widehat{\omega}_k^{(t-1)}$, $1 \leq k \leq L - m$, where extremal values of $\xi\left(\omega, \boldsymbol{a}^{(t-1)}\right)$, defined by (15), occur.
(4) Calculate $\boldsymbol{\Psi}^{(t-1)}$ and $\boldsymbol{\lambda}^{(t-1)}$ using (39).
(5) Determine $\Delta\boldsymbol{a}^{(t)}$, $\delta_p^{(t)}$ and $\delta_s^{(t)}$ using (38) as

$$\begin{bmatrix} \Delta\boldsymbol{a}^{(t)} \\ \delta_p^{(t)} \\ \delta_s^{(t)} \end{bmatrix} = \left(\boldsymbol{\Psi}^{(t-1)}\right)^{-1} \cdot \boldsymbol{\lambda}^{(t-1)}.$$

(6) Update coefficient vector, $\boldsymbol{a}^{(t)} = \boldsymbol{a}^{(t-1)} + \Delta\boldsymbol{a}^{(t)}$.
(7) If $\max\left\{\left|\Delta\boldsymbol{a}^{(t)}\right|, \left|\delta_p^{(t)} - \delta_p^{(t-1)}\right|, \left|\delta_s^{(t)} - \delta_s^{(t-1)}\right|\right\} \leq \Delta_{\text{tol}}$, where $\Delta_{\text{tol}} > 0$ is the prescribed tolerance, jump to the next step, otherwise proceed from step (2).
(8) The end of the algorithm. The unknown coefficient vector $\boldsymbol{a}$ equals $\boldsymbol{a}^{(t)}$, while the weighted Chebyshev norms equals $\delta_p^{(t)}$ and $\delta_s^{(t)}$.

4. Considerations regarding the relative passband magnitude error minimization

In most applications it is usually required that the relative passband magnitude error of the low-pass differentiator is minimised, which means that the weighting function in the passband equals

$$W(\omega) = \frac{1}{\omega}, \quad \omega \leq \omega_p. \tag{40}$$

In this case, the magnitude response error function given by (15) becomes indeterminate for $\omega = 0$. To circumvent this situation, (4), (14) and (40) are substituted in (15) which after employing trigonometric identity

$$\sin\left(\arctan\frac{x}{y}\right) = \frac{x}{\sqrt{x^2 + y^2}},$$

yields the following formulation of the passband magnitude error function:

$$\xi(\omega) = -1 + \frac{\gamma \sum_{n=1}^{L} n a_n \text{sinc}(n\omega)}{\sqrt{\left(1 + \sum_{n=1}^{L} a_n \cos(n\omega)\right)^2 + \left(\sum_{n=1}^{L} a_n \sin(n\omega)\right)^2}}, \quad \omega \leq \omega_p, \tag{41}$$

where

$$\text{sinc}(x) = \begin{cases} \sin x/x, & x \neq 0 \\ 1, & x = 0 \end{cases}. \tag{42}$$

Regarding the lower and upper margin functions of the phase response linearity error, substitution of (40) in (27) yields

$$\mathcal{L}\left(\omega,\,\gamma,\,\delta_p\right)=\arcsin\left[\gamma^{-1}\omega\left(1-\delta_p\right)\right]-\frac{\omega}{\omega_p}\arcsin\left[\gamma^{-1}\omega_p\left(1-\delta_p\right)\right], \tag{43a}$$

$$\mathcal{U}\left(\omega,\,\gamma,\,\delta_p\right)=\arcsin\left[\gamma^{-1}\omega\left(1+\delta_p\right)\right]-\frac{\omega}{\omega_p}\arcsin\left[\gamma^{-1}\omega_p\left(1-\delta_p\right)\right]. \tag{43b}$$

From the previous equations one has

$$\frac{\partial}{\partial\gamma}\mathcal{L}\left(\omega,\,\gamma,\,\delta_p\right)\geq 0, \tag{44a}$$

$$\frac{\partial}{\partial\gamma}\mathcal{U}\left(\omega,\,\gamma,\,\delta_p\right)\leq 0, \tag{44b}$$

which suggests that the passband phase response linearity error decreases with the increase of the parameter γ, assuming the unchanged passband weighted Chebyshev norm δ_p. In a limiting case, that is, when $\gamma^{-1}\omega_p\left(1+\delta_p\right)$ and consequently $\gamma^{-1}\omega_p\left(1-\delta_p\right)$ are small (which is equivalent to $\gamma\gg\omega_p$), the lower and upper margin functions of the passband phase response linearity error reduce to

$$\mathcal{L}\left(\omega,\,\gamma,\,\delta_p\right)\big|_{\gamma\gg\omega_p}=0, \tag{45a}$$

$$\mathcal{U}\left(\omega,\,\gamma,\,\delta_p\right)\big|_{\gamma\gg\omega_p}=2\gamma^{-1}\omega\delta_p\approx 0, \tag{45b}$$

i.e., the passband phase response of the proposed IIR low-pass differentiator is a linear function of frequency regardless the maximum relative passband magnitude error δ_p.

Furthermore, since from (43) it follows that

$$\frac{\partial}{\partial\delta_p}\mathcal{L}\left(\omega,\,\gamma,\,\delta_p\right)\geq 0, \tag{46a}$$

$$\frac{\partial}{\partial\delta_p}\mathcal{U}\left(\omega,\,\gamma,\,\delta_p\right)\geq 0, \tag{46b}$$

if the maximum absolute passband phase response linearity error is required to be below some prescribed value $\overline{\zeta}_\varphi$, while the maximum relative passband magnitude error δ_p is below some $\overline{\delta}_p$, the minimum value of the parameter γ, denoted by γ', can be estimated by solving the following minimization problem

$$\begin{array}{rc} \text{minimise} & \gamma' \\ \text{subject to:} & \gamma'\geq\omega_p\left(1+\overline{\delta}_p\right) \\ & \max\left\{-\min\limits_{\omega\leq\omega_p}\mathcal{L}\left(\omega,\,\gamma',\,0\right),\,\max\limits_{\omega\leq\omega_p}\mathcal{U}\left(\omega,\,\gamma',\,\overline{\delta}_p\right)\right\}=\overline{\zeta}_\varphi \end{array}. \tag{47}$$

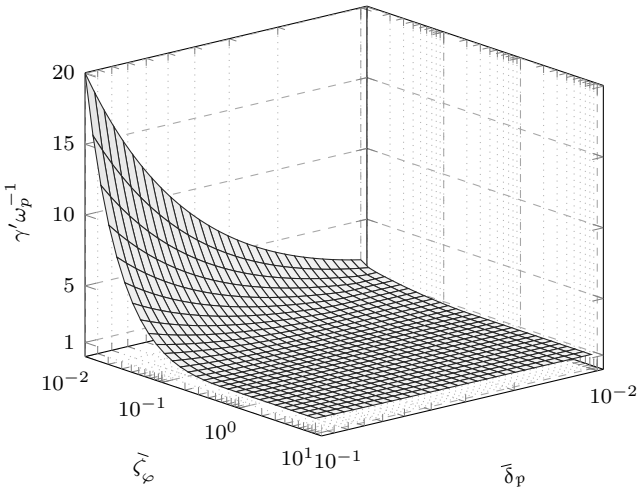

Figure 4. $\gamma'\omega_p^{-1}$ as a function of $\overline{\delta}_p$ and $\overline{\zeta}_\varphi$ for $10^{-2} \leq \overline{\delta}_p \leq 10^{-1}$ and $10^{-2} \leq \overline{\zeta}_\varphi \leq 10$.

Having in mind (44), it can be concluded that the derived optimization problem can be efficiently solved, for example, by using a bisection method. Note that from (43) it follows that the product $\gamma'\omega_p^{-1}$ depends only on $\overline{\delta}_p$ and $\overline{\zeta}_\varphi$. $\gamma'\omega_p^{-1} = f\left(\overline{\delta}_p, \overline{\zeta}_\varphi\right)$ for $10^{-2} \leq \overline{\delta}_p \leq 10^{-1}$ and $10^{-2} \leq \overline{\zeta}_\varphi \leq 10$ is shown in Figure 4. It can be observed that when $\overline{\zeta}_\varphi$ increases and/or $\overline{\delta}_p$ decreases, $\gamma'\omega_p^{-1}$ and consequently γ' decreases.

5. Comparison with the existing IIR low-pass differentiators

In this section, the proposed IIR low-pass differentiators are compared to nearly-linear phase IIR low-pass differentiators from (Al-Alaoui, 2007; Nongpiur et al., 2014). The transfer function of the IIR low-pass differentiators from (Nongpiur et al., 2014) can be expressed as

$$H_1(z) = \left(1 - z^{-1}\right) \frac{\sum_{i=0}^{N-1} p_i z^{-i}}{1 + \sum_{i=1}^{N} q_i z^{-i}}, \tag{48}$$

therefore requiring at least N delays and $2N$ multiplications for realization. On the other hand, the transfer function of the optimised low-pass differentiators from (Al-Alaoui, 2007) takes the following form

$$H_2(z) = \frac{q_0\left(1 - z^{-2}\right)\left(1 + z^{-1}\right)^3}{1 + p_1 z^{-1} + p_2 z^{-2} + p_3 z^{-3} + p_4 z^{-4} + p_5 z^{-5}}, \tag{49}$$

requiring at least 5 delays and 6 multiplications for realization.

As a means of comparison, the maximum relative passband magnitude response error, the average passband group delay, the required number of multiplications and delays, the maximum passband phase response linearity error and average squared

stopband magnitude response defined as in (Nongpiur et al., 2014):

$$P_{sb} = \frac{1}{\pi - \omega_p} \int_{\omega_p}^{\pi} \left| H\left(e^{j\omega}\right) \right|^2 \mathrm{d}\omega, \tag{50}$$

since the methods presented in (Al-Alaoui, 2007; Nongpiur et al., 2014) do not consider the stopband edge frequency, are used. Note that the transfer function (1) of the proposed IIR low-pass differentiators can be realised using $2L$ delays and $L+1$ multiplications. However, if γ is adopted to equal the sum of a few power-of-two terms, the required number of multiplications reduces to L.

In all the examples the passband weighting function required by the proposed design method is given by (40), while in the stopband it equals

$$W(\omega) = 1, \quad \omega \geq \omega_s. \tag{51}$$

The weighted Chebyshev norms, δ_p and δ_s, obtained by utilization of the proposed design method, for some L, ω_p and $W(\omega)$ defined by (40) and (51), depend on γ, m and ω_s. Based on many runs of the proposed design method, the following is observed:

- for the constant L, m and ω_s: when γ increases, δ_p increases while δ_s decreases;
- for the constant L, γ and ω_s: when m decreases, δ_p increases while δ_s decreases;
- for the constant L, γ and m: when ω_s decreases, both δ_p and δ_s increase.

The mentioned observations, along with the conclusions derived in Sec. 4, are fully exploited to set the values of L, m, ω_s and γ, required by the proposed design method, such that the orders of the obtained IIR low-pass differentiators are as low as possible, while the average squared stopband magnitude response defined by (50), the maximum absolute passband phase response linearity and the maximum relative passband magnitude errors are lower than or comparable to those of the existing IIR low-pass differentiators. Additionally, in all the following examples the value of the parameter γ is adopted to equals the sum of a few power-of-two terms; therefore, the required number of multiplications equals the order of the all-pass filter $A_L(z)$. Δ_{tol} in all the examples equals 10^{-10}.

The results of comparison of the proposed IIR low-pass differentiators with those from (Al-Alaoui, 2007; Nongpiur et al., 2014) which have passband edge frequencies equal to 0.29π, 0.3π, 0.4π, 0.5π and 0.7π, along with the adopted values of L, m, γ and ω_s required by the proposed design method, are summarised in Tables 1, 2, 3, 4 and 5, respectively. Corresponding magnitude responses, relative passband magnitude responses and passband phase linearity errors of the existing and proposed IIR low-pass differentiators are given in Figures 5, 6, 7, 8 and 9.

From Tables 1, 2, 3, 4 and 5 it can be observed that the proposed IIR low-pass differentiators for all the considered passband edge frequencies except 0.7π require less multiplications compared to the existing low-pass differentiators from (Al-Alaoui, 2007; Nongpiur et al., 2014). This reduction in the required number of multiplications is significant in cases when passband edge frequencies equal 0.29π, 0.3π and especially 0.5π, where the required number of multiplications equals half the number required by the existing low-pass differentiators. Furthermore, the proposed IIR low-pass differentiators exhibit considerably lower passband phase response linearity errors compared to the existing differentiators from (Al-Alaoui, 2007; Nongpiur et al., 2014) for all passband edge frequencies except 0.5π, note Figures 5C, 6C, 7C, 8C and 9C and Tables 1, 2, 3, 4 and 5. The average squared stopband magnitude response of

Table 1. $\omega_p = 0.29\pi$. Comparison between the proposed IIR low-pass differentiator and the existing one from (Nongpiur et al., 2014).

Parameters	Proposed $L = 6$, $m = 3$, $\gamma = 4$, $\omega_s = 0.45\pi$	Method in (Nongpiur et al., 2014)
Filter order	12	4
δ_p	0.012	0.015
P_{sb}	0.17	0.16
$\overline{\tau}$	5.75	3.70
$\max_{\omega \le \omega_p} \lvert\zeta_\varphi(\omega)\rvert$ in degrees	0.24	1.45
no. of multiplications	6	8
no. of delays	12	4

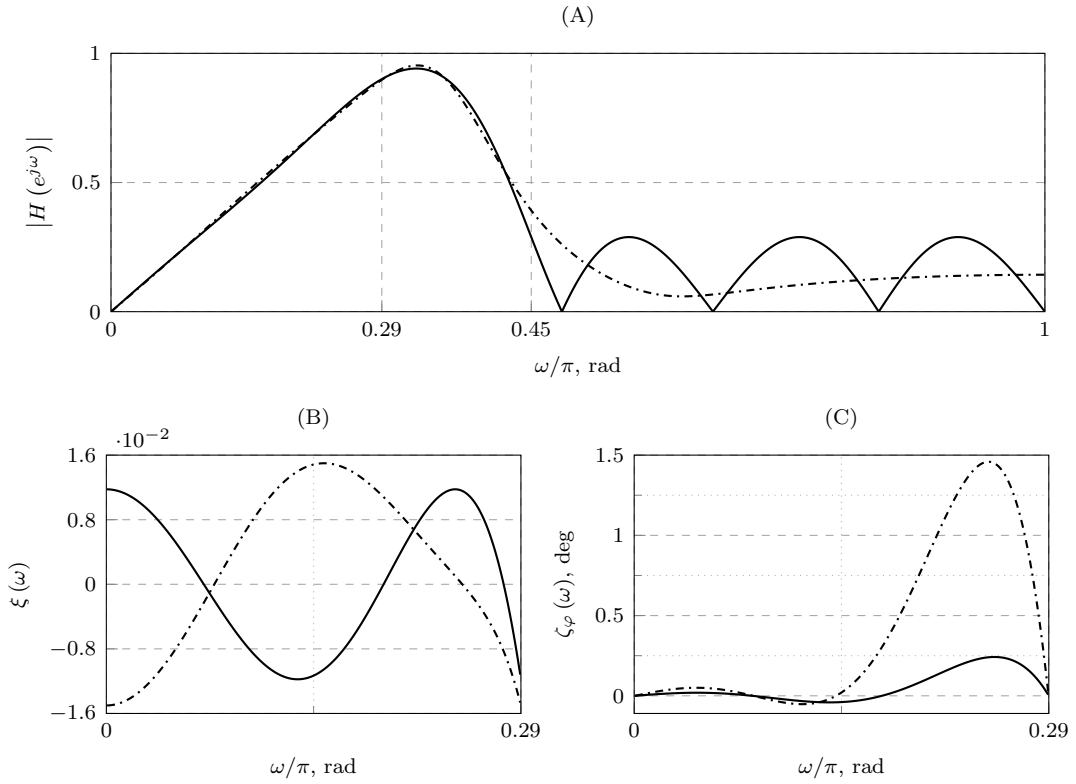

Figure 5. $\omega_p = 0.29\pi$. (A) Magnitude responses, (B) relative passband magnitude response errors and (C) passband phase response linearity errors of the IIR low-pass differentiator from (Nongpiur et al., 2014) (dash dot lines) and the proposed one (solid lines).

Table 2. $\omega_p = 0.3\pi$. Comparison between the proposed IIR low-pass differentiator and the existing ones from (Al-Alaoui, 2007; Nongpiur et al., 2014).

Parameters	Proposed $L = 4$, $m = 2$, $\gamma = 2.5$, $\omega_s = 0.57\pi$	Method in (Nongpiur et al., 2014)	Method in (Al-Alaoui, 2007)
Filter order	8	3	5
δ_p	0.024	0.035	0.026
P_{sb}	0.24	0.23	0.24
$\overline{\tau}$	3.6	3.36	2.34
$\max_{\omega \le \omega_p} \lvert\zeta_\varphi(\omega)\rvert$ in degrees	0.62	1.08	6.27
no. of multiplications	4	6	6
no. of delays	8	3	5

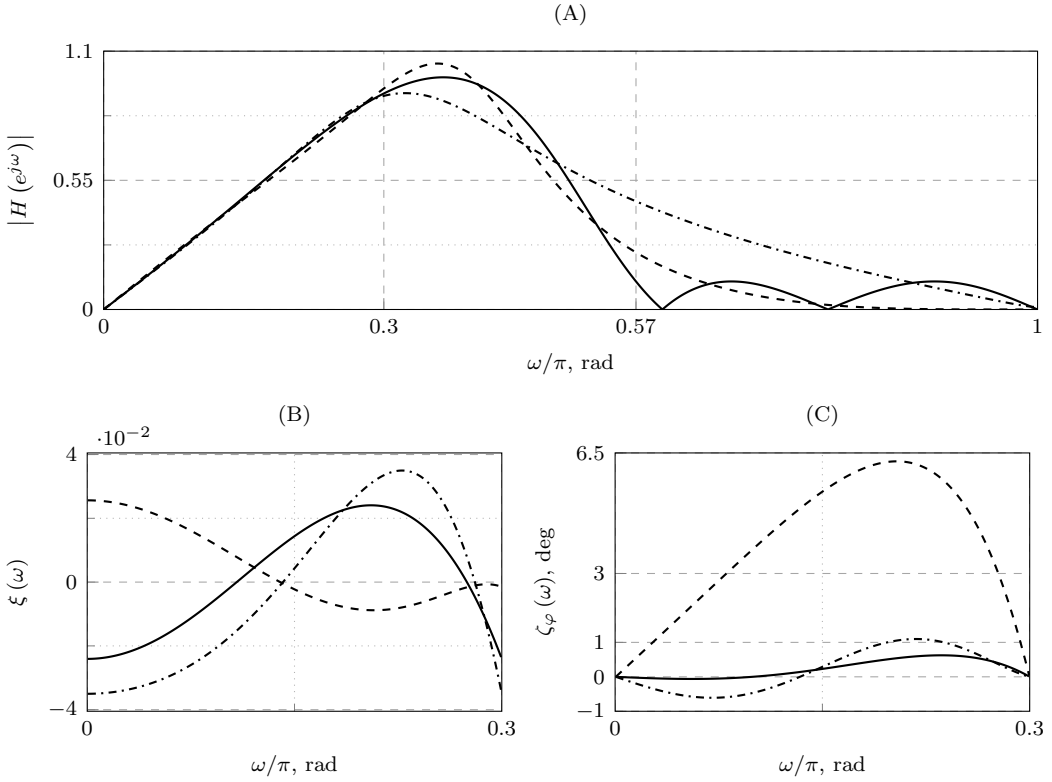

Figure 6. $\omega_p = 0.3\pi$. (A) Magnitude responses, (B) relative passband magnitude response errors and (C) passband phase response linearity errors of the IIR low-pass differentiator from (Nongpiur et al., 2014) (dash dot line), (Al-Alaoui, 2007) (dashed lines) and the proposed one (solid lines).

Table 3. $\omega_p = 0.4\pi$. Comparison between the proposed IIR low-pass differentiator and the existing one from (Al-Alaoui, 2007).

Parameters	Proposed $L = 5$, $m = 3$, $\gamma = 2.5$, $\omega_s = 0.6\pi$	Method in (Al-Alaoui, 2007)
Filter order	10	5
δ_p	0.01	0.02
P_{sb}	0.39	0.41
$\overline{\tau}$	4.59	1.98
$\max_{\omega \le \omega_p} \lvert\zeta_\varphi(\omega)\rvert$ in degrees	0.5	10.58
no. of multiplications	5	6
no. of delays	10	5

Table 4. $\omega_p = 0.5\pi$. Comparison between the proposed IIR low-pass differentiator and the existing ones from (Al-Alaoui, 2007; Nongpiur et al., 2014).

Parameters	Proposed $L = 3$, $m = 2, \gamma = 2$, $\omega_s = 0.725\pi$	Method in (Nongpiur et al., 2014)	Method in (Al-Alaoui, 2007)
Filter order	6	3	5
δ_p	0.04	0.06	0.07
P_{sb}	0.83	0.88	0.89
$\overline{\tau}$	2.45	2.31	1.66
$\max_{\omega \le \omega_p} \lvert\zeta_\varphi(\omega)\rvert$ in degrees	1.21	1.06	11.77
no. of multiplications	3	6	6
no. of delays	6	3	5

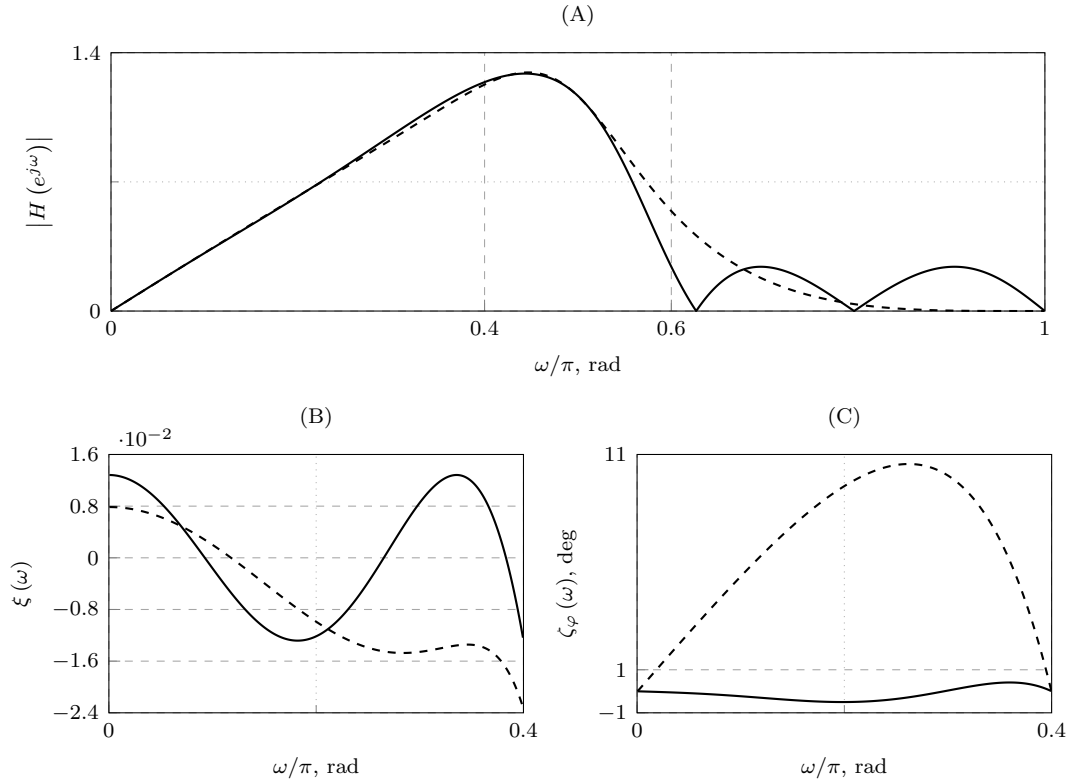

Figure 7. $\omega_p = 0.4\pi$. (A) Magnitude responses, (B) relative passband magnitude response errors and (C) passband phase response linearity errors of the IIR low-pass differentiator from (Al-Alaoui, 2007) (dashed lines) and the proposed one (solid lines).

Table 5. $\omega_p = 0.7\pi$. Comparison between the proposed IIR low-pass differentiator and the existing one from (Nongpiur et al., 2014).

Parameters	Proposed $L = 9$, $m = 7$, $\gamma = 2.5$, $\omega_s = 0.825\pi$	Method in (Nongpiur et al., 2014)
Filter order	18	4
δ_p	0.008	0.01
P_{sb}	1.14	1.2
$\overline{\tau}$	8.52	2.02
$\max_{\omega \le \omega_p} \lvert\zeta_\varphi(\omega)\rvert$ in degrees	4.61	11.74
no. of multiplications	9	8
no. of delays	18	4

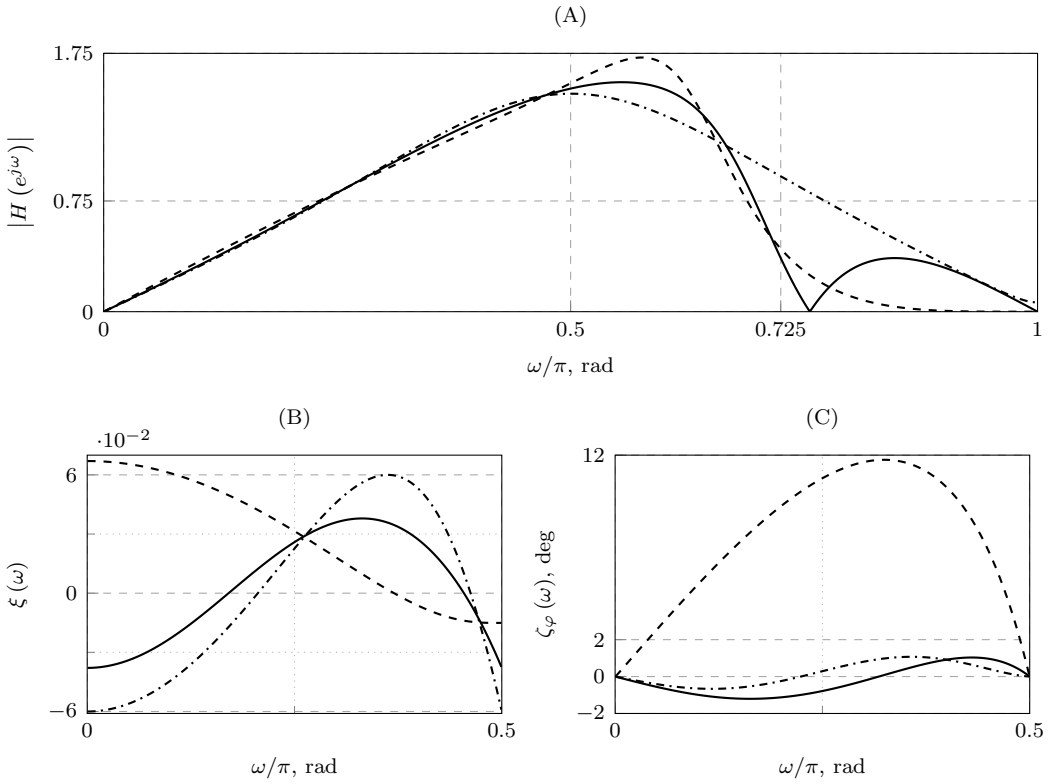

Figure 8. $\omega_p = 0.5\pi$. (A) Magnitude responses, (B) relative passband magnitude response errors and (C) passband phase response linearity errors of the IIR low-pass differentiator from (Nongpiur et al., 2014) (dash dot line), (Al-Alaoui, 2007) (dashed lines) and the proposed one (solid lines).

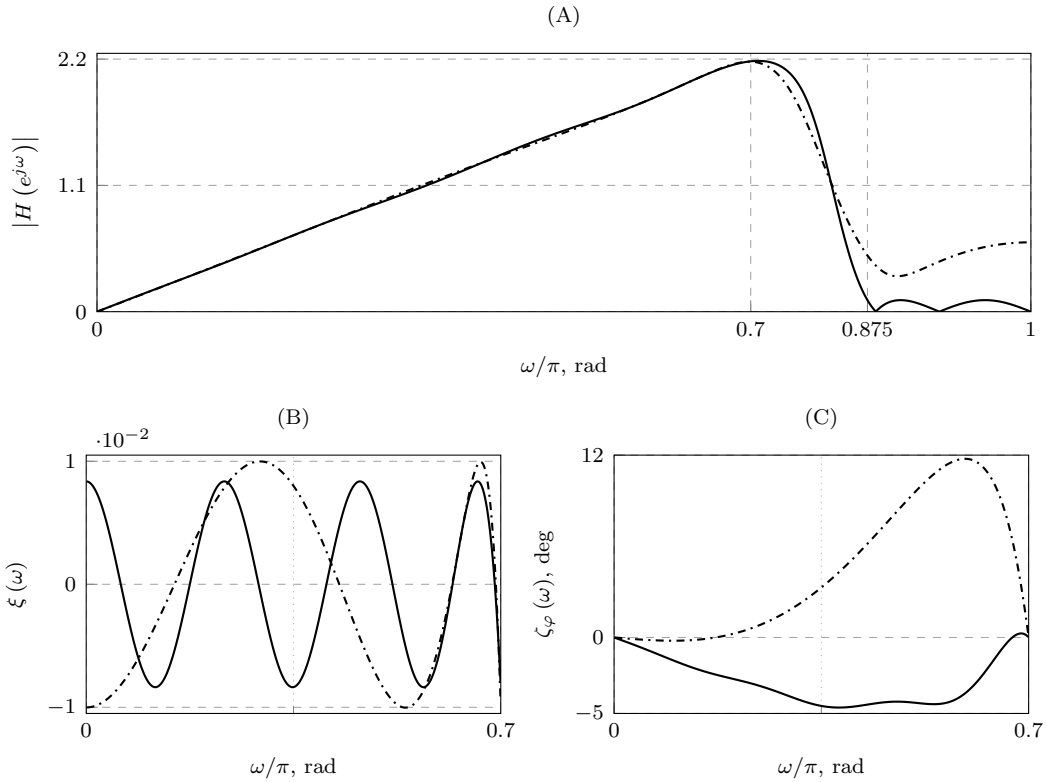

Figure 9. $\omega_p = 0.7\pi$. (A) Magnitude responses, (B) relative passband magnitude response errors and (C) passband phase response linearity errors of the IIR low-pass differentiator from (Nongpiur et al., 2014) (dash dot lines) and the proposed one (solid lines).

Table 6. Poles of the proposed nearly-linear phase IIR low-pass differentiators competing with the existing ones from (Al-Alaoui, 2007; Nongpiur et al., 2014).

ω_p				
0.29π	0.3π	0.4π	0.5π	0.7π
$0.6262 \cdot e^{\pm j0.8222\pi}$	0.3260	$0.6145 \cdot e^{j\pi}$	0.2516	$0.7146 \cdot e^{j\pi}$
$0.6421 \cdot e^{\pm j0.4522\pi}$	$0.4938 \cdot e^{j\pi}$	$0.7023 \cdot e^{\pm j0.5737\pi}$	$0.7448 \cdot e^{\pm j0.7016\pi}$	$0.8666 \cdot e^{\pm j0.7827\pi}$
$0.4311 \cdot e^{\pm j0.1380\pi}$	$0.5986 \cdot e^{\pm j0.5125\pi}$	$0.3725 \cdot e^{\pm j0.1784\pi}$		$0.5822 \cdot e^{\pm j0.5449\pi}$
				$0.5292 \cdot e^{\pm j0.3178\pi}$
				$0.4964 \cdot e^{\pm j0.1024\pi}$

the obtained low-pass differentiators, for all considered passband edge frequencies, is lower or comparable to those of the existing IIR low-pass differentiators. The poles of the IIR low-pass differentiators obtained by utilization of the proposed design method are given in Table 6.

Increased orders of the proposed IIR low-pass differentiators in all the examples, and consequently a higher group delay response, reflects the existance of the term z^{-L} in the transfer function of the proposed nearly-linear phase low-pass differentiators, note (1). However, if the hardware implementation is considered and if the proposed IIR low-pass differentiators require less multiplications compared to the existing ones, which leads to lower power consumption, the proposed all-pass-based IIR low-pass differentiators present an attractive alternative in applications where low passband group delay is not required.

6. Conclusion

The novelty of the paper is the introduction of a new structure for the nearly-linear phase IIR low-pass differentiators design composed of two parallel all-pass filters of the same orders, where one of the all-pass branches is a pure delay. The magnitude and phase responses of the proposed differentiators are shown to be related, such that by controlling the value of the maximum passband magnitude response and the value of the parameter γ, the passband phase response linearity error can also be effectively controlled. The utilization of the proposed design method results in a transfer function with a magnitude response approximating the ideal one in the weighted Chebyshev sense both in the passband and the stopband. The order of the proposed IIR low-pass differentiators equals double the order of the all-pass filter in one of the parallel branches, while the required number of multiplications equals the order of the all-pass filter if γ is adopted to equal the sum of a few power-of-two terms.

The results of the comparison show that although the minimum number of delays required by the proposed IIR low-pass differentiators (with comparable or lower average squared magnitude responses, maximum absolute passband phase response linearity and maximum relative passband magnitude errors) is obviously greater compared to the existing nearly-linear phase IIR low-pass differentiators, the required number of multiplications is usually decreased. This, if hardware implementation were to be considered, leads to lower power consumption, making the proposed all-pass-based IIR low-pass differentiators an attractive alternative in applications where the low passband group delay is not required.

Acknowledgement

This work was supported by the Ministry of Education, Science and Technological Development of the Republic of Serbia under the project TR33035.

References

Al-Alaoui, M. A. (1995). A class of second-order integrators and low-pass differentiators. *IEEE Transactions on Circuits and Systems I: Fundamental Theory and Applications*, *42*(4), 220–223.

Al-Alaoui, M. A. (2007). Linear phase low-pass IIR digital differentiators. *IEEE Transactions on signal processing*, *55*(2), 697–706.

Ferdi, Y. (2010). Improved lowpass differentiator for physiological signal processing. In *2010 7th International Symposium on Communication Systems, Networks & Digital Signal Processing (CSNDSP 2010)*, 747–750.

Khan, I. R., Okuda, M., & Ohba, R. (2005). Digital differentiators for narrow band applications in the lower to midband range. In *2005 IEEE International Symposium on Circuits and Systems*, 3721–3724.

Kumar, B., & Roy, S. D. (1988). Design of digital differentiators for low frequencies. *Proceedings of the IEEE*, *76*(3), 287–289.

Laguna, P., Thakor, N. V., Caminal, P., & Jane, R. (1990). Low-pass differentiators for biological signals with known spectra: application to ECG signal processing. *IEEE transactions on biomedical engineering*, *37*(4), 420–425.

Le Bihan, (J. 1993). Novel class of digital integrators and differentiators. *Electronics Letters*, *29*(11), 971–973.

Luo, J., Bai, J., He, P., & Ying, K. (2004). Axial strain calculation using a low-pass digital differentiator in ultrasound elastography. *IEEE transactions on ultrasonics, ferroelectrics, and frequency control*, *51*(9), 1119–1127.

Nakamoto, M., & Ohno, S. (2014). Design of Multi-Band Digital Filters and Full-Band Digital Differentiators Without Frequency Sampling and Iterative Optimization. *IEEE Transactions on Industrial Electronics*, *61*(9), 4857–4866.

Nongpiur, R. C., Shpak, D. J., & Antoniou, A. (2014). Design of IIR digital differentiators using constrained optimization. *IEEE Trans. Signal Processing*, *62*(7), 1729–1739.

de la O Serna, J. A., & Platas-Garza, M. A. (2011). Maximally flat differentiators through WLS Taylor decomposition. *Digital Signal Processing*, *21*(2), 183–194.

Platas-Garza, M. A., Platas-Garza, J., & de la O Serna, J. A. (2009). Dynamic phasor and frequency estimates through maximally flat differentiators. *IEEE Transactions on instrumentation and measurement*, *59*(7), 1803–1811.

Selesnick, I. W. (2002). Maximally flat low-pass digital differentiator. *IEEE Transactions on Circuits and Systems II: Analog and Digital Signal Processing*, *49*(3), 219–223.

Skogstad, S. A., Holm, S., & Høvin, M. (2012). Designing digital IIR low-pass differentiators with multi-objective optimization. In *2012 IEEE 11th International Conference on Signal Processing*, *1*, 10–15.

Skolnik, M. I. (1980). Introduction to radar systems. *New York, McGraw Hill Book Co., 1980. 590 p.*.

Stančić, G., Krstić, I., & Živković, M. (2019). Design of IIR fullband differentiators using parallel all-pass structure. *Digital Signal Processing*, *87*, 132 – 144.

Väliviita, S., & Ovaska, S. J. (1998). Delayless recursive differentiator with efficient noise attenuation for control instrumentation. *Signal Processing*, *69*(3), 267–280.

Wang, Y. (2013). New window functions for the design of narrowband lowpass differentiators. *Circuits, Systems, and Signal Processing*, *32*(4), 1771–1790.

Wulf, M., Staude, G., Knopp, A., & Felderhoff, T. (2016). Efficient design of FIR filter based

low-pass differentiators for biomedical signal processing. *Current Directions in Biomedical Engineering*, *2*(1), 215–219.

Yoshida, T., Nakamoto, M., & Aikawa, N. (2018). Low-delay and high-functioning digital differentiators in the big data era. *Electronics and Communications in Japan*, *101*(10), 31–37.